

is the dimensionless vorticity,  $\bar{u} = ur_0^2/Q$  is the dimensionless longitudinal component of the velocity vector,  $\bar{v} = vr_0^2/Q$  is the dimensionless radial component of the velocity vector,  $\bar{p} = p/(\rho u_{\text{mean}}^2)$  is the dimensionless pressure,  $\Delta\bar{p}_0$  is the dimensionless pressure drop in a CT,  $\Delta\bar{p}$  is the dimensionless pressure drop in a TVC,  $C_f = \tau_w/(\rho u_{\text{mean}}^2/2)$  is the local friction resistance coefficient,  $\lambda_f$  is the friction resistance coefficient,  $\lambda_e$  is the pressure resistance coefficient,  $\lambda_t$  is the total resistance coefficient in a TVC,  $\lambda_0$  is the resistance of a CT,  $\bar{\lambda}_t = \lambda_t/\lambda_0$  is the ratio of the total TVC resistance to the CT resistance,  $\bar{\lambda}_f = \lambda_f/\lambda_0$  is the ratio of the TVC friction resistance to the CT resistance, and  $\bar{\lambda}_e = \lambda_e/\lambda_0$  denotes the ratio of the TVC pressure resistance to the CT resistance.

#### LITERATURE CITED

1. I. L. Povkh, Technical Hydromechanics [in Russian], Leningrad (1976).
2. I. L. Povkh, N. V. Finoshin, and V. V. Gutnik, "Numerical flow studies in tubes of varying cross section," UkrNIInti, No. 1652, 10/10/86, Donetsk (1986).
3. I. L. Povkh and N. V. Finoshin, Teor. Prikl. Mekh., No. 21, 120-124, Khar'kov (1990).
4. I. L. Povkh, in: Physical Hydrodynamics [in Russian], Donetsk (1989), pp. 16-20.
5. J. A. Deiber and W. R. Showalter, AIChE J., 25, No. 4, 638-648 (1972).

#### DISTRIBUTION OF VOLUME-AVERAGED PARAMETERS OF VORTEX FLOW OVER THE ENERGY SEPARATION CHAMBER OF A VORTEX TUBE WITH SUPPLEMENTED FLOW

Sh. A. Piralishvili and V. M. Kudryavtsev

UDC 621.565.3/088.8

*The profiles of averaged circular and axial velocity components, temperature, and pressure are measured in the axisymmetric channel of the energy separation chamber of a vortex tube with the introduction of additional flow in the near-axis zone on the side cross section where throttle is located.*

In a series of engineering devices (vortex burners, plasma production apparatus, vortex igniters, and projected power equipment), the preferred, and sometimes the only method for controlling the mass and heat transfer is to sharply whirl the flow as it flows along an axisymmetric channel. Vortex flow in the energy separation chambers of vortex tubes is one of the most complex and incompletely understood methods. While the gas dynamics of counterflow separation vortex tubes is known [1, 2], there are no publications of such investigations of double-contour tubes. At the same time, knowledge of the nature of the distribution of thermodynamics and kinematic flow parameters is important for developing an adequate physical and mathematical model, in order to perfect further the energy separation processes in these tubes. This is even more important because today these tubes have the highest adiabatic efficiency, as computed from the overall characteristics of the process for cooling part of the gas. In some tubes the cooled gas mass flow exceeds the initial flow [2, 3].

The investigation was conducted on a unit whose working section was a conical axisymmetric vortex tube with a minimum diameter of the separation chamber  $d_1 = 0.03$  m and with a cone angle  $\gamma = 15^\circ$ ; the relative length of the energy separation chamber was  $\bar{l} = L/d_1 = 9$ . The relative area of the nozzle input  $\bar{F}_n = F_n/F_{tr}$  was measured from 0.02 to 0.1 in

tests. The optimum value of  $\bar{F}_n$  depended on the pressure at the input to the nozzle of the vortex generator. Thus for  $P_1^* = 0.4$  MPa,  $\bar{F}_{n \text{ opt}} = 0.04$ . A derotational slit diffuser, whose dimensions were optimized according to recommendations in [2, 3], was mounted on the end of the tube opposite the nozzle input. The test stand was supplied with compressed air through a nozzle input to the vortex generator within the tube, and supplemental flow at an intermediate pressure was introduced through a connecting tube located in the near-axis zone of the slit diffuser. The equipment allowed measurement and automatic recording of the parameters at the input and the outputs, and also in the control sections. An electronic digital pulse transformer (ÉVIP-16) connected to a computer allowed the data to be reduced with the use of a specially developed program. The temperature transducers were Chromel–Copel and copper–constantan thermocouples with wire diameters of 0.5 mm and 0.1 mm, respectively. Pitot tubes were used to pick up the total pressures. The pressure was measured using manometers with an accuracy class of 0.5. In order to automate the measurements miniature transducers with electrical output signals (MD-10, MD-2, and MDD-1-1000 of accuracy class 1.0) were used. The flows were measured with the use of a throttling orifice and flow-metering nozzles, which were calibrated at the All-Union Metrological Institute. The accuracy class was 1.8.

The velocity field was measured dynamically by using a three-channel probe to measure the total and static pressures and the dynamic pressure differences. The characteristics of the average flow were investigated using methods discussed in [1, 4], considering recommendations in [5-7].

The miniature combined probe was a thin polished plate, welded from three stainless steel tubes 0.4 mm diameter. The height of the working part of the probe is 25 mm. The distance from the forward edge (the point for measuring the total pressure) to the orifice for measuring the static pressure is 1.1 mm. The diameters of the three input openings of the probe are  $d = 0.12$  mm. When the transducer is completely immersed in the flow, the area of its central cross section did not exceed 1.4% of the area of the transverse cross section of the vortex tube. The transducer was calibrated by a method discussed in [7], with the aid of a nozzle designed from Vitoshinskii's formula. In order to calibrate the probe in the supersonic region, a Laval nozzle was used, the constricted part of which was profiled according to Vitoshinskii's formula [7] and the supersonic part was calculated from the formula [6]

$$F/F_{cr} = (1 + 0,2M^2)^{3/1,73M}, \quad (1)$$

where  $F_{cr}$  is the area of the critical cross section.

The thermocouples were calibrated both statically and dynamically. In order to measure the total temperature, a copper–constantan thermocouple was used, which was placed in a cylindrical sheath made of stainless steel. During the experiment the relative flow of the cooled flow  $\mu = G_c/G_1$  was varied, where  $G_1$  is the mass flow of the compressed gas passing through the nozzle of the vortex generator, and the pressure at the input to the tube was  $P_1^* = 0.3-0.5$  MPa. The measurements were done in six sections equally spaced along the length of the energy separation chamber at the following values of the dimensionless longitudinal coordinate  $\bar{z} = z/d_1 = 1.7(n + 1.43)$ , where  $n = 0, 1, 2, 3, 4$ , and 5. The experimental results are shown in Figs. 1 and 2.

The nature of the distribution of the total and static parameters, which represent the aerodynamic flow picture (Fig. 1) lead to the following conclusions: In the double-contour vortex tube (the vortex tube with supplemental flow) flows are predominately opposite the direction of the vortex: a peripheral flow which moves from the input nozzle to the throttle, and a near-axis flow whose axial velocity is in the reverse direction. The nature of the pressure distribution and the axial velocity in section VI leads to the conclusion that the assumption  $G_c = G_s$  is correct for operating regimes of the tube where the efficiency of the energy separation reaches a maximum ( $G_s$  is the additional gas flow introduced from the side of the throttle into the near-axis zone of the tube). Judging from experimental data, the near-axis forced vortex is formed mainly from elements of gas which are introduced supplementally. The actual distribution of averaged flow parameters is substantially nonuniform over the volume of the tube, both over its length and over its cross section. The radial gradients of the static pressure and the total temperature decrease along the length of the tube from the section of the nozzle input to the section where the throttle is located. The maximum radial pressure gradients are observed in the nozzle section. The distribution of the tangential and axial velocities are qualitatively similar for various cross sections, which verifies the assumption of the self-similarity of the flow in the development of an adequate physical-mathematical model of the phenomenon. The circular velocities are greatly reduced as the throttle is moved. By analyzing the nature of the pressure and velocity distribution and by noting the substantial reduction of the gradients along the length of the tube, it can be concluded that it is desirable to shorten the length of the energy separation chamber of the vortex tube with a supplemental flow up to  $l = 5-6$  without reducing the efficiency characteristics of the redistribution process of the total enthalpy. Experiments [2, 3] confirm this conclusion.

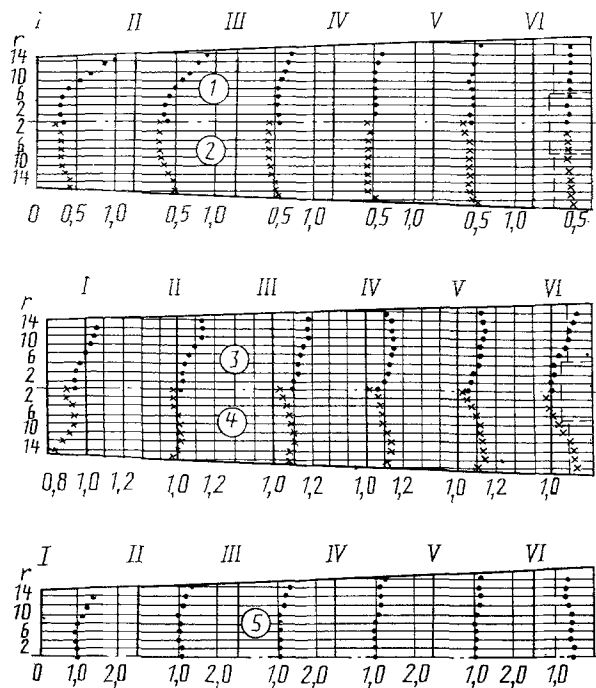


Fig. 1. Distribution of parameters over the volume of the vortex tube: 1)  $P^*/P_1^*$ ; 2)  $P/P_1^*$ ; 3)  $\Theta^* = T^*/T_1^*$ ; 4)  $\Theta = T/T_1$ ; 5)  $\rho/\rho_1$ .  $T_1^* = T_s^* = 293$  K;  $P_1^* = 0.4$  MPa;  $P_s^* = 0.14$  MPa;  $\mu = 1.6$ ; I-IV are the cross sections where the transducer was located.

In studying the flow in vortex tubes it is important to know where the maxima of the circular velocity and the zero of the axial components occur in the cross section. According to the vortex interaction hypothesis, the maximum of  $V_\varphi$  and the point where  $V_z = 0$  coincide in a cross section perpendicular to the axis of symmetry. This is the so-called radius of vortex separation:  $\bar{r}_2 = r_2/r_1$ . As can be seen from the nature of the velocity distribution along the axis of the tube, it can be stated from an experimental viewpoint that this coincidence takes place. The surface of vortex separation,  $r_2 = \text{const}$ , is almost cylindrical.

The intensity of the whirling of the peripheral vortex decreases along the length of the tube from the nozzle input to the throttle ( $V_\varphi = 0$ ). On the other hand, the near-axis flow is transformed from an axial flow on the side of the throttle to a whirling flow as the flow goes towards the opening in the diaphragm which is located in the cross section next to the nozzle input. The whirling becomes more intensive as the relative fraction of the cooled flow is increased, that is, as the relative mass of gas elements which are introduced supplementally into the near-axis zone of the tube from the side of the throttle becomes larger.

The distribution of the axial velocity component along the tube for various cross sections with various relative coordinates is shown in Fig. 2a. It can be noted that the magnitude of the axial velocity component of the near-axis forced vortex for a fixed relative fraction of cooled flow is practically unchanged along the energy separation chamber in the case where the flow is formed from elements of supplementally introduced gas. Here an equality  $G_c \approx G_s$  should be observed. When it is not, in particular when  $G_c > G_s$ , the process of forming the forced near-axis vortex becomes more complicated, because it also includes elements of the peripheral quasipotential vortex, which occurs in practice along the energy separation chamber. Probably this explains the divergence in the numerical values of the axial velocity in various sections of the vortex tube. Thus, closer to the nozzle input, the axial velocity increases, which is related to the growth of the gas flow through a cylindrical channel with a radius equal to the radius of vortex separation  $\bar{r}_2$ .

The insignificant deviation of the [location of the] maximum of the circular velocity component from the radius where the axial velocity is zero (Fig. 2b), which does not exceed the experimental accuracy, does not contradict the basic hypothesis of vortex interaction. Some deviation of the function  $V_\varphi(r)$  from the potential-vortex law should be related to the effect of conditions at the solid wall and to obvious methodological experimental errors, which are related to the fact that the dynamic methods for experimentally determining the velocities in turbulent flows are always accompanied by systematic errors, which arise from pulsating components of the velocities. However, when a physical-mathematical model is constructed which uses

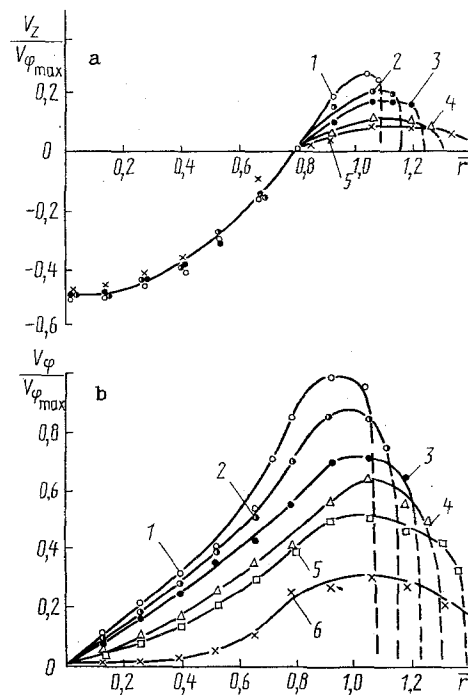


Fig. 2. Distribution of the axial (a) and circular (b) velocity components: 1)  $z = 1.7$ ; 2)  $z = 3.13$ ; 3)  $z = 4.56$ ; 4)  $z = 5.99$ ; 5)  $z = 7.42$ ; 6)  $z = 8.85$ .  $T_1^* = T_s^* = 293$  K;  $P_1^* = 0.5$  MPa;  $P_s^* = 0.14$  MPa;  $\mu = 1.6$ ;  $V_{\varphi 1} = 335$  m/sec.

integral methods, it can be assumed that the flow in the peripheral vortex is a potential flow  $V_{\varphi} r = \text{const}$ . This is also justified by the insignificant radial extent of the region of potential flow  $0.8 < \bar{r} < 1.0$ . The nature of the velocity profile in the near-axis vortex  $0 < \bar{r} < \bar{r}_2$  is close to the rotation of a solid body  $\omega = \text{const}$ . An interesting experimental result indicates the practical independence of the vortex separation radius  $\bar{r}_2 = 0.8$  on the relative fraction of cooled flow. The profile of the axial velocity components for  $\mu = 1.6$  and  $\mu = 1.0$  passes through zero at the same radius  $\bar{r} = 0.8$  over the whole length of the tube (Fig. 2a). There is practically no effect on this radius from the pressure of the compressed gas at the nozzle input of the vortex generator of the vortex tube. Obviously this result cannot be used in developing a physical-mathematical model by assuming that the relative vortex separation radius is  $\bar{r}_2 = 0.8$  for a critical flow regime from the opening of the diaphragm  $M_z = 1$ . The physical explanation of this result obviously is that the process for forming the aerodynamics and the redistribution of the total enthalpy is affected mainly by the nature of the turbulent flow and the intensity of the turbulence, which in the range of these experiments is practically constant.

The level of free turbulence for operating conditions of the vortex tube in the experiment was estimated by calculation to be  $\varepsilon = 25.8\%$ . Here the level of near-wall turbulence did not exceed  $\varepsilon = 5.1-7\%$ . The calculations were conducted for a Reynolds number computed from the chamber diameter of the energy separation chamber of the vortex tube in its nozzle section  $d_1$  and the maximum of the circular velocity  $V_{\varphi 1}$  at the input to the energy separation chamber, that is, at the output of the nozzle of the vortex generator. For the experimental conditions, the value of the Reynolds number was within the limits of  $10^5-10^6$ .

## NOTATION

$d_1$  – diameter (m) of the energy separation chamber in the nozzle section of the vortex tube;  $\gamma$  – cone angle;  $L$  (m) – length of the energy separation chamber;  $\bar{l}$  – relative length of the energy separation chamber;  $F$  (m<sup>2</sup>) – cross-sectional area;  $M$  – Mach number;  $G$  (kg/sec) – mass flow;  $\mu$  – relative fraction of the cooled flow;  $P$  (MPa) – pressure of the compressed gas;  $\bar{P} = P/P_1$  and  $\bar{P}^* = P^*/P_1^*$  – reduced pressures;  $z$  (m) – longitudinal coordinate;  $n$  – a parameter;  $V$  (m/sec) – velocity;  $\bar{V}_{\varphi} = V_{\varphi}/V_{\varphi 1}$ ,  $\bar{V}_z = V_z/V_{\varphi 1}$  – dimensionless velocities;  $\Theta$  – relative dimensionless temperature;  $r$  (m) – radius;  $\bar{r} = r/r_1$  – dimensionless radius;  $\rho$  (kg/m<sup>3</sup>) – density;  $\bar{\rho} = \rho/\rho_1$  – relative density;  $A$  – an experimental coefficient; and  $\omega$  (sec<sup>-1</sup>) – angular velocity. Indices: 1 – at the input to the input nozzle of the vortex tube; 2 – at the

separation radius of the vortices; c – cooled flow; h – heated flow; s – supplemented flow; cr – critical cross section; \* – deceleration parameter; z – axial component;  $\varphi$  – circular component; r – radial component; st – static parameter; meas – measurement; ' – pulsed component.

## LITERATURE CITED

1. A. P. Merkulov, The Vortex Effect and Its Application in Engineering [in Russian], Moscow (1969).
2. A. D. Suslov, S. V. Ivanov, A. V. Murashkin, et al., Vortex Apparatus [in Russian], Moscow (1985).
3. Sh. A. Piraliashvili and V. G. Mikhailov, in: Some Problems of Investigating Heat Transfer and Thermal Machines [in Russian], No. 56, Kuibyshev (1973), pp. 64-74.
4. A. P. Merkulov and N. D. Kolyshev, Trans. Kuibyshev Aviation Inst., No. 22, pp. 18-24, Kuibyshev (1965).
5. I. O. Khintse, Turbulence [in Russian], Moscow (1963).
6. G. N. Abramovich, Applied Gas Dynamics [in Russian], Moscow (1975).
7. N. F. Krasnov (ed.), Applied Aerodynamics [in Russian], Moscow (1974).

## CALCULATION OF THE CHARACTERISTICS OF PARTICLES IN INHOMOGENEOUS TURBULENT STREAMS

I. V. Derevich

UDC 532.529

*The influence of inertia, averaged phase slip, and inhomogeneity of the turbulent carrier stream on the parameters of the disperse phase in the flow of a gas suspension in a round pipe is investigated on the basis of a closed system of equations for the first and second moments of particle velocity pulsations.*

The averaged characteristics of a disperse phase (particle concentration, average velocity) depend essentially on the intensity of the pulsating motion of the particles. The pulsation energy of the disperse phase is determined by three main factors. The first is the particle inertia, equal to the ratio of the time of dynamic relaxation of particles to the integrated macroscopic time scale of turbulence of the carrier stream. As the time of dynamic relaxation of the particles decreases, the pulsation energy of the discrete phase approaches that of the carrier phase. An increase in the time of dynamic relaxation of the particles in comparison with the lifetime of energy-carrying vortices decreases the degree of entrainment of particles in the pulsating motion. The influence of particle inertia on the pulsation characteristics of a disperse admixture in a homogeneous turbulent stream has been well studied, in [1, 2], for example.

Second, in particle flow under the conditions of averaged velocity slip, an effect of "crossing of trajectories" of particles and turbulent floats arises. As a result of the continuous renewal of turbulent floats crossing a particle trajectory, the autocorrelation function of pulsations of gas velocity along a particle trajectory decays faster than the original autocorrelation function of gas velocity pulsations, leading to a decrease in the intensity of pulsating motion of the discrete admixture and to a decrease in the turbulent diffusion coefficient of the particles. In the case of isotropic turbulence, the action of the averaged velocity slip of the phases on the pulsation characteristics of the particles has been investigated both experimentally and theoretically in [3-8].

---

G. M. Krzhizhanovskii Scientific-Research Power Institute, Moscow. Translated from *Inzhenerno-Fizicheskii Zhurnal*, Vol. 62, No. 4, pp. 539-545, April, 1992. Original article submitted June 10, 1991.